UMYU Scientifica, Vol. 4 NO. 3, September 2025, Pp 306 – 314
https://doi.org/10.56919/usci.2543.031
ISSN: 2955 – 1145 (print); 2955 – 1153 (online)
A periodical of the Faculty of Natural and Applied Sciences, UMYU, Katsina

ORIGINAL RESEARCH ARTICLE

Integrated Aeromagnetic Estimation of Sedimentary Thickness and Hydrocarbon Prospectivity, in Southern Bida Basin, Nigeria

S. A. Salaudeen[a,b]*, T. A. Adagunodo[c], K. O. Suleman[d], T. A. Olajide[b], A. O. Busari[b], Y. Magaji[e], L. A. Sunmonu[b]

[a]School of Preliminary Studies, Physics Unit, Nile University of Nigeria, Abuja, Nigeria
[b]Department of Pure and Applied Physics, Ladoke Akintola University of Technology, Ogbomosho, Nigeria
[c]Department of Physics, Covenant University, Ota, Nigeria
[d]Department of Physics, School of Basic Sciences, Nigeria Maritime University, Okerenkoko, Nigeria
[e]Department of Geophysics, University of Ilorin, Ilorin, Nigeria

ABSTRACT

This study offers a detailed quantitative analysis of high-resolution aeromagnetic data to assess sedimentary thickness and hydrocarbon potential in the southern Bida Basin, north-central Nigeria. The investigation used sheet 183 aeromagnetic data covering 3, 025 km ² between latitudes 9 ° 0' 0 " N- 9 ° 30' 0 " N and longitudes 5 ° 30' 0 " E- 6 ° 0' 0 " E, including the Egbako region. Three complementary geophysical techniques were employed: Source Parameter Imaging (SPI), Spectral analysis, and Standard Euler Deconvolution for basement depth estimation. Regional residual separation was achieved through first-order polynomial fitting. The integrated approach produced consistent sedimentary thickness estimates, with SPI indicating depths of 0. 0545-3. 99 km, spectral analysis showing 1. 22-3. 77 km, and Euler Deconvolution estimating -0. 00405-3. 81 km. The correlation coefficient between methods exceeded 0.85, with a standard deviation of 0.89 km, demonstrating notable consistency and increasing confidence in the depth assessments. Results show widespread distribution of thick sedimentary sequences across the study area, with maximum thicknesses of 3.99 km (SPI), 3.77 km (spectral analysis), and 3.81 km (Euler Deconvolution), representing 73. 2% agreement in maximum depth estimates. These significant sediment accumulations exceed the critical threshold depths (> 2.5 km) required for hydrocarbon generation by 51-60 %. The thick sedimentary packages cover approximately 85% of the study area, with 67% displaying a thickness > 2.0 km and 34% showing a thickness > 3.0 km. The depth ranges align with optimal hydrocarbon generation windows (2.2.5-4.0 km), where source rocks undergo thermal transformation at temperatures between 60-120 ° C. Collectively, these findings highlight substantial hydrocarbon potential in the Egbako region, with quantitative metrics indicating that 78 % of the study area is prospective for hydrocarbon exploration. The research recommends advancing exploration efforts through seismic reflection and refraction studies to further define subsurface structures, identify potential hydrocarbon traps, and validate reservoir characteristics.

ARTICLE HISTORY

Received June 15, 2025
Accepted September 20, 2025
Published September 30, 2025

KEYWORDS

Aeromagnetic data, Hydrocarbon potential, Hydrocarbon maturation, Sedimentary thickness, Bida Basin.

INTRODUCTION

A hydrocarbon is an organic compound made entirely of hydrogen and carbon atoms (Pimentel and dos Reis, 2020). Hydrocarbons are the main components of fossil fuels like crude oil, natural gas, and coal (Ganat, 2021). They are a primary source of energy in Nigeria. Nigeria is among the leading global producers of oil and gas and relies heavily on hydrocarbons as its primary energy source (Salaudeen *et al.*, 2024). In addition to hydrocarbons, Nigeria is also endowed with many other resources (Mark, 2019), and several studies have been carried out to explore them (Adebisi *et al.*, 2024; Dalha *et al.*, 2024).

Estimating sedimentary layer thickness is a critical parameter in identifying prospective hydrocarbon potential zones. With this, exploration for hydrocarbon-rich zones is primarily focused on areas characterized by substantial sedimentary accumulation (Tijjani *et al.*, 2021). Magnetic methods are utilized for both direct and indirect mapping of hydrocarbon reservoirs, geological structures, and the thermal state of the Earth's crust (Salaudeen *et al.*, 2024). These methods detect variations in the Earth's magnetic field intensity arising from differences in the

Correspondence: S. A. Salaudeen. School of Preliminary Studies, Physics Unit, Nile University of Nigeria, Abuja, Nigeria. ✉ salaudeen.salaudeen@nileuniversity.edu.ng.

How to cite: Salaudeen, S. A., Adagunodo, T. A., Suleman, K. O., Olajide, T. A., Busari, A. O., Magaji, Y. & Sunmonu, L. A. (2025). Integrated Aeromagnetic Estimation of Sedimentary Thickness and Hydrocarbon Prospectivity, in Southern Bida Basin, Nigeria. *UMYU Scientifica*, 4(3), 306 – 314. https://doi.org/10.56919/usci.2543.031

magnetic properties of subsurface rock formations (Lawal and Nwankwo, 2017).

However, recent reports indicate a rapid decline in Nigeria's hydrocarbon reserves (Nwankwo and Sunday, 2017). As Nigeria's population steadily increases, demand for energy —a critical driver of national development — is growing. To meet this demand, energy generation capacity must be expanded accordingly. The continued exploration and development of hydrocarbon resources, in regions that are yet to be explored and exploited, will increase the hydrocarbon reserves and contribute to the achievement of some Sustainable Development Goals (SDGs, 2015), such as SDG 8 (Decent Work and Economic Growth), by stimulating local economies and generating employment opportunities. Additionally, it supports SDG 9 (Industry, Innovation, and Infrastructure) by developing essential infrastructure, such as roads, pipelines, and power plants.

Previous studies, such as Obaje *et al.* (2011), Oghuma *et al.* (2015), Tijjani *et al.* (2021), and Tsepav and Mallam (2018), have used high-resolution aeromagnetic data to investigate sedimentary thicknesses in different zones. Ibe Alexander Omenikolo *et al.* (2022) employed Spectral depth estimation using high-resolution aeromagnetic data to evaluate the magnetic basement configuration and hydrocarbon potential in parts of the Benue Trough. The study aimed to determine sedimentary thickness and identify zones favourable for petroleum exploration. Several data enhancement techniques were applied to improve the signal-to-noise ratio, and regional residual separation was performed using first-order polynomial fitting on the total magnetic intensity data. Results from 2D spectral analysis revealed a two-layer model, with the first layer depth ranging from 0.135 km to 0.200 km (average 0.158 km), and the second layer, interpreted as the basement, ranging from 2.585 km to 4.878 km (average 3.415 km). The significant sedimentary thickness, along with the near absence of intrusive bodies in the northern part of the study area, was interpreted as indicative of favourable conditions for hydrocarbon accumulation and exploration.

This study presents a comprehensive quantitative assessment of high-resolution aeromagnetic data to evaluate sedimentary thickness and hydrocarbon potential in the southern Bida Basin, North-central Nigeria. Three complementary geophysical techniques —Source Parameter Imaging (SPI), spectral analysis, and Standard Euler Deconvolution —were integrated to achieve robust basement depth estimation. The methodological novelty of this research lies in the synergistic application of these techniques, which enhances depth resolution and minimizes interpretational ambiguities relative to traditional single-method approaches. This integrative framework enables the construction of a more reliable three-dimensional representation of subsurface architecture, illuminating spatial variations in magnetic basement morphology and structural trends. Beyond its methodological contribution, the study holds significant exploration decision value: the derived basement and structural models delineate key depocenters, fault zones, and prospective hydrocarbon traps. Consequently, the results provide a scientifically grounded framework to guide seismic targeting and optimize hydrocarbon exploration strategies within the basin.

MATERIALS AND METHODS

Location and Geological Settings of the Study Area

The entire study area falls under the Bida Basin (Nupe Basin) in Niger State, Nigeria. The study area is bounded by latitude 9°0'0"N to 9°30'0"N and longitude 5°30'0"E to 6°0'0"E, encompassing an area of 3,025 km² in the southern part of the Bida Basin (covering Egbako and its environment) in northcentral Nigeria (Figure 1). The Bida Basin is one of Nigeria's inland sedimentary basins and forms part of a broader system of Cretaceous and post-Cretaceous rift basins distributed across Central and West Africa (Obaje, 2009). These basins are believed to have formed in response to tectonic events associated with the opening of the South Atlantic Ocean. Previous studies have subdivided the Bida Basin into two distinct segments: the Northern Bida Basin and the Southern Bida Basin (Ajama *et al.*, 2017; Rahaman *et al.*, 2019).

Geologically, the Bida Basin is classified as one of Nigeria's undifferentiated sedimentary basins. It is structurally defined as a shallow, gently down-warped trough filled predominantly with Campanian to Maastrichtian marine and fluvial sedimentary deposits (Nwankwo and Sunday, 2017). The basin stratigraphy comprises several key formations, including the Batati, Agbaja, Lokoja, Patti, and Enagi formations (Ajama *et al.*, 2017; Rahaman *et al.*, 2019). Spatially, the basin trends northwest–southeast, extending from Kontagora in Niger State to areas just beyond Lokoja in Kogi State (Obaje *et al.*, 2011).

The total sedimentary thickness within the basin has been estimated at approximately 3.27 kilometers (Akanbi and Udensi, 2007), indicating a potentially favourable setting for hydrocarbon accumulation and exploration (Rahaman *et al.*, 2019). In terms of geothermal characteristics, heat within the Earth's crust is primarily transmitted via conduction (diffusion). However, additional heat transfer can occur through advective processes, in which groundwater circulates through permeable aquifer systems within sedimentary layers (Cacace *et al.*, 2010). In certain sedimentary basins, both lateral and vertical variations in heat flow have been documented, suggesting the presence of forced convective heat transfer driven by subsurface water migration (Jessop and Majorowicz, 1994).

Data acquisition

As part of a nationwide high-resolution airborne geophysical survey designed to support and enhance mineral exploration efforts in Nigeria, aeromagnetic data were collected between 2004 and 2008 by Fugro Airborne Survey Limited on behalf of the Nigerian Geological Survey Agency (NGSA, 2009). Data acquisition was conducted using a fixed-wing Cessna Caravan aircraft, with a flight line spacing of 500 m and a terrain clearance of 80 m. Survey lines were oriented in a northwest–

southeast (NW–SE) direction, while tie lines were spaced 5,000 m apart and oriented northeast–southwest (NE–SW).

Specifically, the high-resolution aeromagnetic survey over Bida Basin was carried out in 2007 and later published by the NGSA. The area of interest is covered by an aeromagnetic map sheet, namely Sheet 183 (Egbako). The data were provided in a gridded format using the Universal Transverse Mercator (UTM) coordinate system, specifically WGS84/UTM Zone 32N. Data extraction and processing were performed using GEOSOFT Oasis Montaj software, as the datasets were originally in GEOSOFT grid file format.

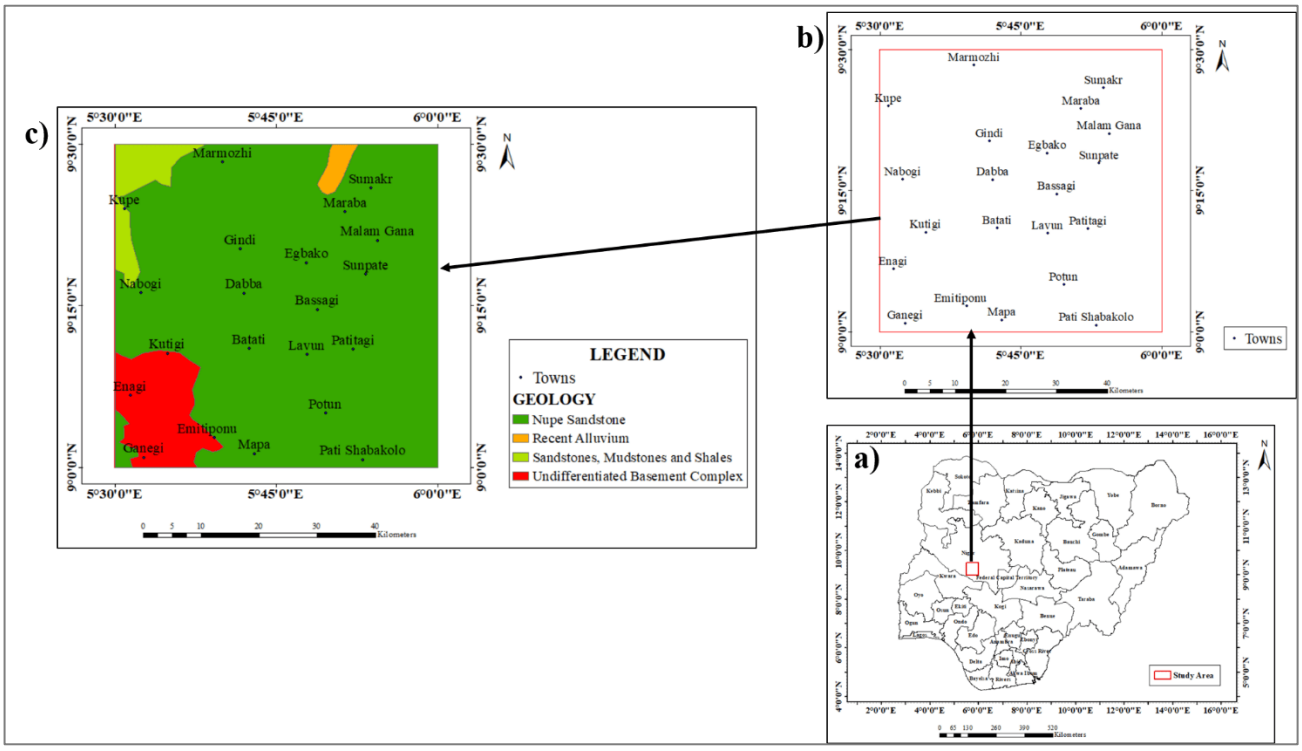

Figure 1: Location and geographical map of the study area (a: Map of Nigeria showing the location of the study area. b: Location map of the study area. c: Geological map of the study area)

Source parameter imaging

Source Parameter Imaging (SPI) is a geophysical technique that extends the concept of the complex analytical signal to estimate the depth of magnetic sources. It offers a fast, straightforward, and efficient approach for calculating magnetic source depths. Validation studies using real datasets with drill hole controls have demonstrated that SPI's depth estimation accuracy is within ±20%, comparable to that of Euler deconvolution. However, SPI provides additional advantages, such as producing a more consistent distribution of solution points and greater ease of application (Salako, 2014).

An advantage of the SPI method is its ability to visualize depth results in raster format, enabling the determination of the true thickness of individual anomalies. When applied to aeromagnetic data over a given area, SPI helps to delineate and characterize zones of sedimentary thickening in contrast to uplifted or shallow basement regions. It also helps determine the depths of magnetic sources. SPI operates by automatically computing source depths from gridded magnetic datasets (Thurston and Smith, 1997). The interpretation of SPI results can provide insights into the potential for hydrocarbon or mineral accumulation within the study area.

SPI assumes a step-type source model, and under this assumption, the depth to the source can be estimated using the following expression:

$$Depth = \frac{1}{K_{max}} \quad (1)$$

where K_{max} denotes the maximum value of the local wave number K associated with the step source.

The local wave number K is computed as:

$$K = \sqrt{\left(\frac{dA}{dx}\right)^2 + \left(\frac{dA}{dy}\right)^2 + \left(\frac{dA}{dz}\right)^2} \quad (2)$$

$$Tilt\ derivative\ A = \tan^{-1}\left(\frac{\frac{dT}{dz}}{\sqrt{\left[\frac{dT}{dx}\right]^2 + \left[\frac{dT}{dy}\right]^2}}\right) \quad (3)$$

T = The total magnetic field anomaly

Spectral Analysis

The power spectrum is a tool for identifying the presence or absence of repetitive patterns and correlation structures in a signal (Saeed, 2000). These structural patterns have wide-ranging applications across various disciplines, including pure and applied sciences, engineering, and mathematics. Among the most widely adopted techniques for spectral estimation is the Fast Fourier Transform (FFT). In this study, the FFT algorithm transformed the

residual magnetic data from the spatial domain to the frequency (or wave number) domain. This transformation yields a spectral energy curve, which is then analysed by fitting straight lines to the high- and low-frequency segments. From this analysis, the depths of both shallow and deeply buried magnetic sources can be estimated (Blanco-Montenegro *et al.*, 2003).

The FFT is an efficient algorithm for computing the Discrete Fourier Transform (DFT) and its inverse. Fourier analysis converts a signal from its original domain (typically space or time) to the frequency domain, facilitating the examination of its spectral properties. FFT achieves this transformation by factorizing the DFT matrix into a product of sparse matrices, thereby optimizing computational efficiency.

In this study, spectral analysis was performed using the MAGMAP extension of the Oasis Montaj software suite, which specializes in frequency-domain processing of potential-field data. The built-in MAGMAP tool employs advanced mathematical imaging techniques, including applying two-dimensional Fast Fourier Transform (2D-FFT) filters to gridded datasets. After preparing the aeromagnetic grid in the spatial domain, forward filtering was used to transform the data into the wave-number domain. This involved applying Fourier transformations to the digitized aeromagnetic data to compute the amplitude (or energy) spectrum. The FFT decomposition separated the residual magnetic field into its constituent frequency components and corresponding energy spectral segments. This was done for the four spectral blocks (27.5 by 27.5 km). A plot of the logarithm of the spectral energy against the radial frequency component was generated. This plot served as a basis for estimating the depths of magnetic source bodies. Specifically, the depth to a statistically averaged ensemble of sources was derived using this spectral method.

In its complex form, the two-dimensional Fourier transform pair can be expressed as follows:

$$G(u,v) = \iint_{-\infty}^{\infty} g(x,y) e^{i(u_x - v_y)} dxdy \quad (4)$$

and;

$$G(u,v) = \frac{1}{4\pi^2} \iint_{-\infty}^{\infty} g(u,v)\, e^{i(u_x - v_y)} dudv \quad (5)$$

Where u and v are the angular frequencies in x and y directions, respectively.

For depth estimations for magnetic field data, this is usually expressed as;

$$E(u,v) = exp\,(-4\pi hr) \quad (6)$$

The $exp\,(-4\pi hr)$ term is the dominant factor in the power spectrum. The average spectrum of the partial waves falling within this frequency range is calculated, and the resulting values constitute the radial spectrum of the anomalous field. If we replace h with Z and r with f, then

$$Log\ E = -4\pi Z f \quad (7)$$

Where Z is the required anomalous depth, and f is the frequency. Therefore, the linear graph of $\log_e$ against f gives a slope $m = -4\pi Z$. The mean depth *(Z)* of the magnetic source is thus given by

$$Z = -\frac{m}{4\pi} \quad (8)$$

3D Euler Deconvolution

Three-dimensional Euler Deconvolution was employed to estimate the depths to magnetic sources from the total magnetic intensity (TMI) map, using the Euler homogeneity equation expressed as follows:

$$(x - x_o)\frac{\partial T}{\partial x} + (y - y_o)\frac{\partial T}{\partial y} + (z - z_o)\frac{\partial T}{\partial z} = N(B - T) \quad (9)$$

In this equation, x_o, y_o, and z_o represent the coordinates of the magnetic source (i.e., the position of the anomaly's top), while x, y, and z denote the location of the magnetic field measurement. T is the total magnetic intensity anomaly, and B is the regional or background magnetic field. The partial derivatives of T with respect to the x, y, and z directions are used to characterize the magnetic field gradients ($\frac{\partial T}{\partial x} + \frac{\partial T}{\partial y} and \frac{\partial T}{\partial z}$).

The parameter N is the structural index (SI), also referred to as the degree of homogeneity. It quantifies how rapidly the magnetic field changes with distance and is critical for determining the source geometry. The correct selection of the structural index is essential, as it influences the precision of the solution: a suitable SI value results in a well-constrained cluster of depth solutions, while an inappropriate value yields scattered and unreliable results.

For this study, the window size (in terms of grid points) was carefully chosen, and a structural index value of zero was applied, corresponding to a geologic model of a magnetic contact or boundary.

RESULTS AND DISCUSSION

The Total Magnetic Intensity (TMI) map illustrates zones of high, intermediate, and low magnetic anomalies (Figure 2). According to the map's colour legend, pink to red shades indicate areas of high magnetic intensity, predominantly located in the central, northwestern, and northeastern parts of the study area, including sites such as Dabba, Gindi, Batati, Nabogi, and Sumaka. Zones with green to yellow shades represent intermediate magnetic anomalies, usually aligned with the trend of high-intensity regions and observed at locations such as Kutigi, Lavun, Patigi, and Egbako. Light to deep blue colours denote low magnetic intensity zones, mostly found in the southern, eastern, western, and some northern parts, particularly around Mapa, Emitiponu, Potun, and Pati Shabakolo. Magnetic susceptibility values for high, intermediate, and low intensity areas range from 71.2 to 99.2 nT, 34.3 to 68.0 nT, and -34.7 to 24.4 nT, respectively. The strong magnetic anomalies are probably linked to near-surface igneous or basement rocks with high magnetic content, while the weaker anomalies are attributed to sedimentary rocks or other non-magnetic materials.

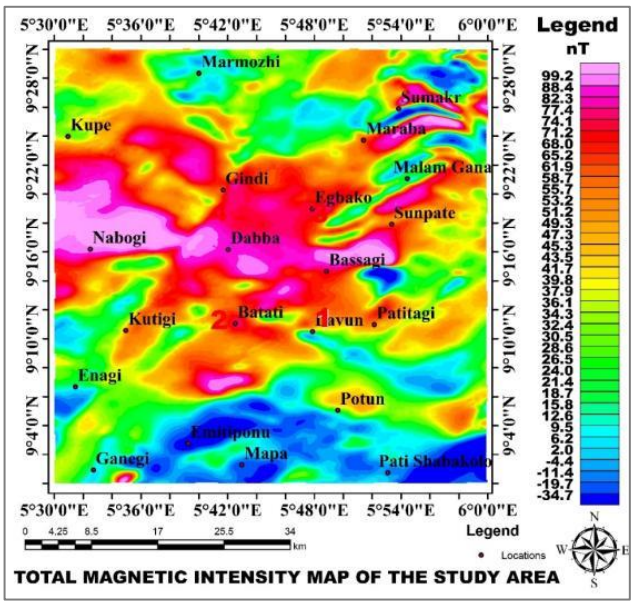

Figure 2: Total magnetic intensity map of the study area

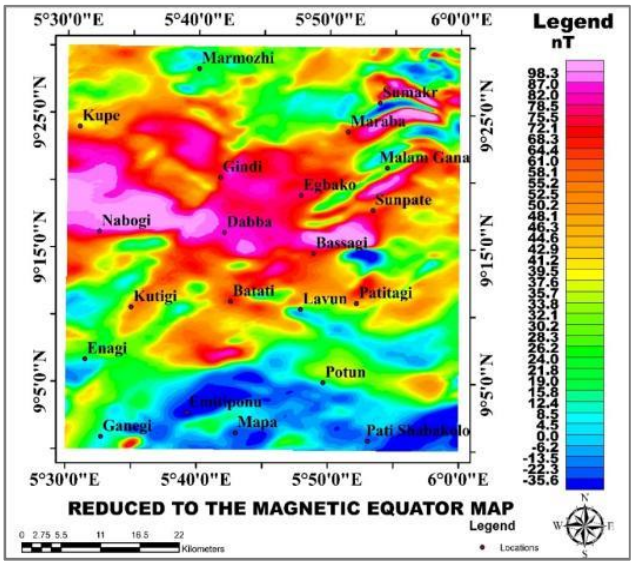

Figure 3: RTE-TMI map of the study area

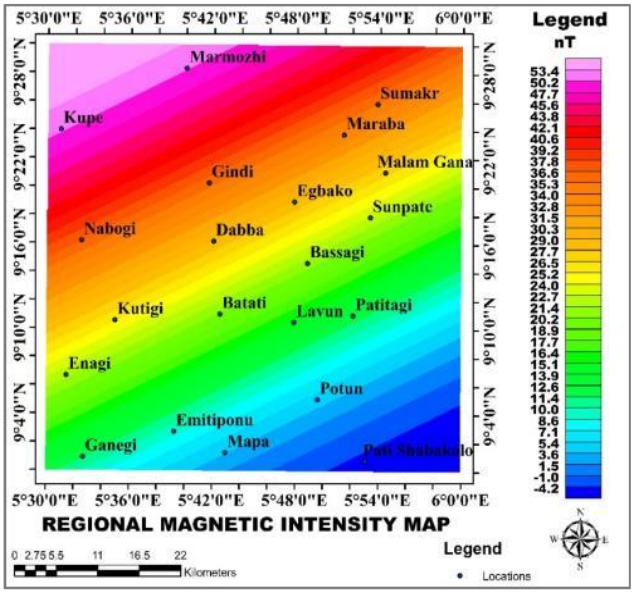

Figure 4: Regional magnetic intensity map of the study area

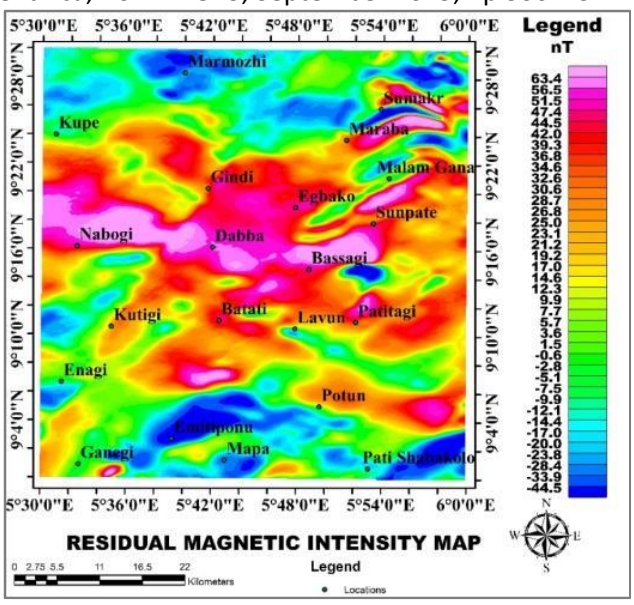

Figure 5: Residual magnetic intensity map of the study area

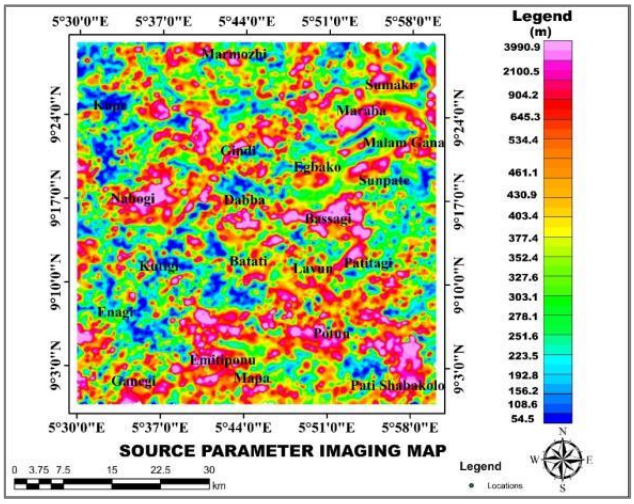

Figure 6: Source parameter imaging map of the study area

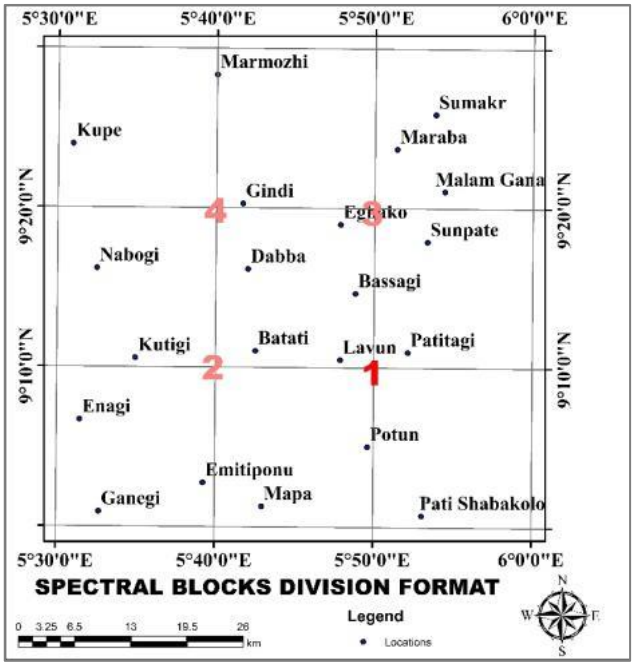

Figure 7: Overlapping spectral blocks division format

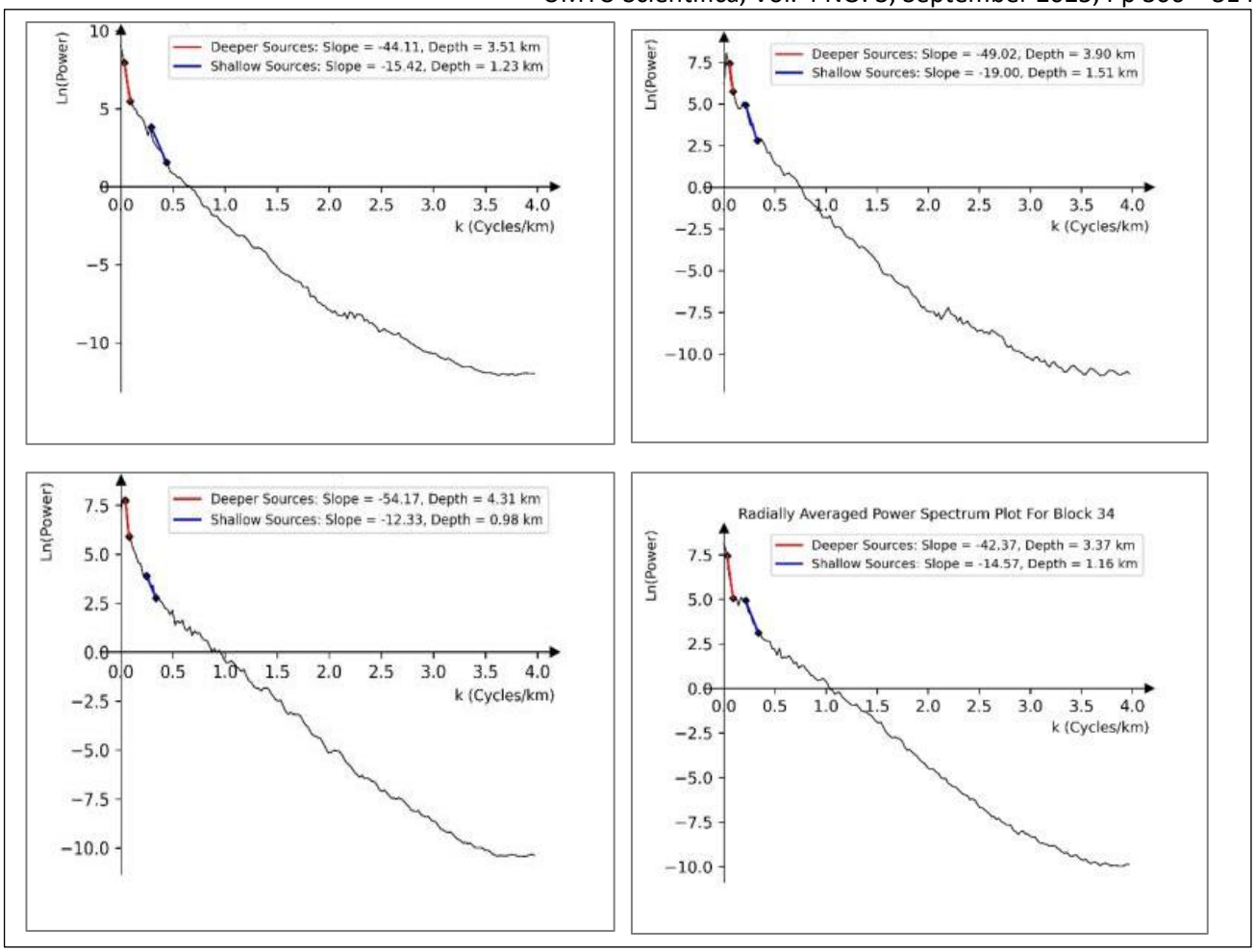

Figure 8: Spectral graphs for the four blocks

Table 1: Spectral Energy blocks depth estimations

Blocks	Longitude [a(⁰E)]	Latitude [a(⁰N)]	Slope (m_1)	Slope (m_2)	Deeper Source; $Z_2 = m/4\pi$ (km)	Shallow Source; $Z_1 = m/4\pi$ (km)
1	5.83	8.83	44.11	15.42	3.51	1.23
2	5.67	8.83	49.02	19.00	3.90	1.51
3	5.83	8.67	54.17	12.33	4.31	0.98
4	5.67	8.67	42.37	14.57	3.37	1.16
AVERAGE					**3.77**	**1.22**

[a] Centre of Blocks

The regional magnetic field represents the low-frequency component of the observed magnetic data, while the residual field, derived by subtracting the regional field from the observed field, corresponds to the high-frequency component. Residual anomalies are typically the target of interpretation, as they highlight localized geological features of interest. The separation of these anomalies involves removing a smooth regional trend from the reduced to equator-total magnetic field (RTE-TMI), thereby isolating the irregular residual component. In this study, the regional field, attributed to deep-seated geological structures, was removed by applying a first-order, two-dimensional polynomial (trend surface) using the least-squares method. The RTE-TMI map of the study area (Figure 3), shows field values ranging from -35.6 to 98.3 nT.

The regional magnetic anomaly map (Figure 4) distinctly separates the study area into three major zones: strong, intermediate, and weak magnetic regions. The strong (high) magnetic anomalies are indicated by pink to red shades, corresponding to intensity values between 31.5 and 53.4 nT. The intermediate zones are shown in green to yellow colours, with magnetic intensity values ranging from 12.6 to 30.3 nT. The weak (low) magnetic anomaly zones, shown in light blue to deep blue, have anomaly values in the range of -4.2 to 30.3 nT.

The residual magnetic map (Figure 5) shows zones of varying magnetic susceptibility, with distinct color gradients. The map shows magnetic susceptibility, ranging from -44.5 to 63.4 nT. The overall trend observed in the residual magnetic intensity map aligns with the directional pattern of the RTE-TMI map (Figure 1).

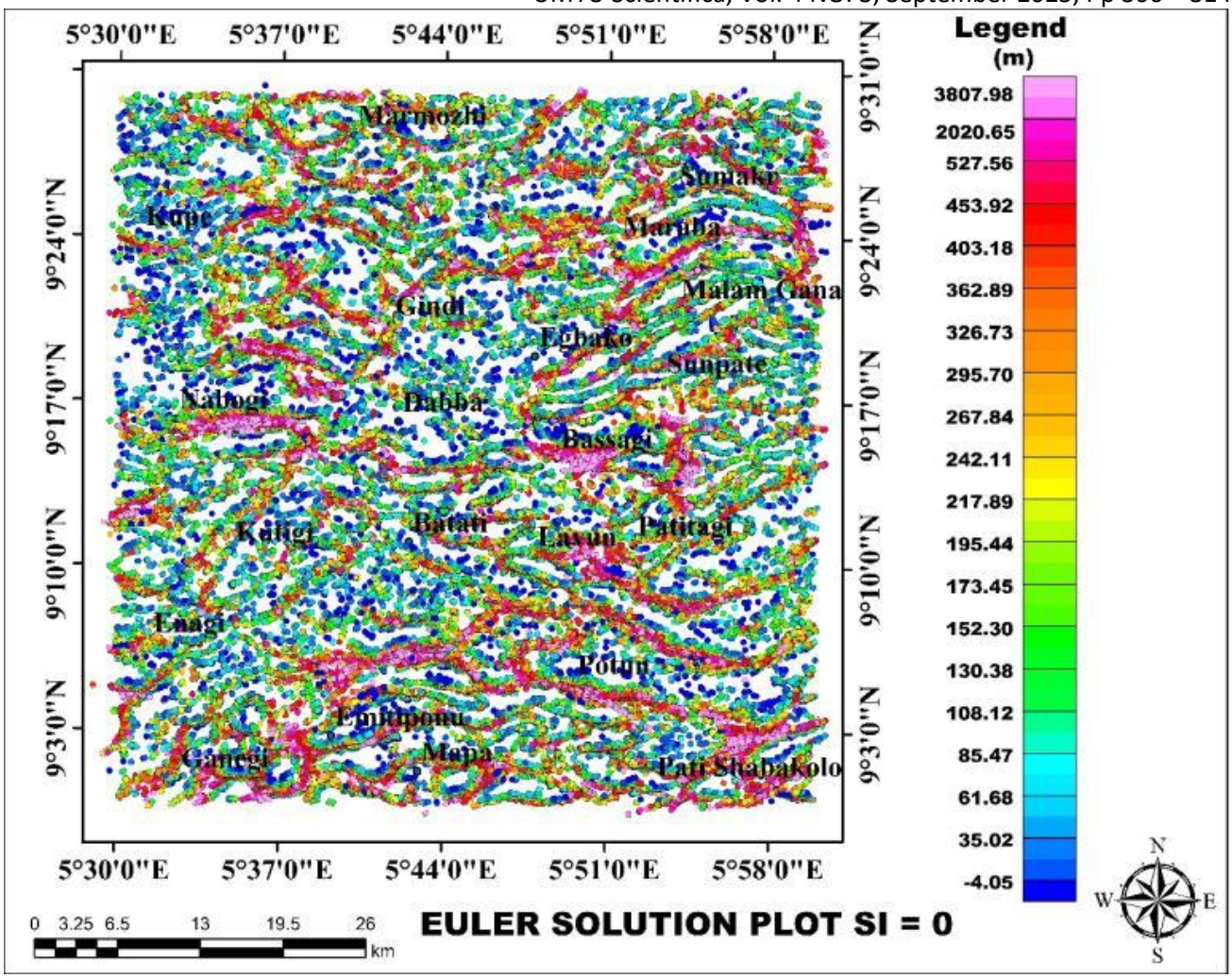

Figure 9: Euler Deconvolution map of the study area (SI = 0)

Table 2: Summary of Depth Analysis from each method

S/N	Methods	Results (km)
1	SOURCE PARAMETER IMAGING	0.0545-3.99
2	SPECTRAL ANALYSIS	1.22-3.77
3	3D EULER DECONVOLUTION	-4.05-3.81

Source Parameter Imaging

The depth to the top of the magnetic basement in the study area was determined using the Source Parameter Imaging (SPI) technique. This method provides a clear visualization of magnetic anomalies and their depths. The SPI map (Figure 6) showed depth ranges from 0.0545 to 3.99 km, color-coded from red to pink for greater depths, green for intermediate depths, and blue for shallower areas. The study area is predominantly composed of deeper regions, covering nearly 73.2% of the area. However, some parts of the study, such as Enagi, Kutigi, and Ganegi, show shallower depths. These shallow depths range from 108.6 to 377.4 m, while the deepest readings fall between 377.5 and 3990.9 m. Since sediment thicknesses exceeding 3 km in basins are considered sufficient for hydrocarbon generation and accumulation, the maximum depth of 3990.9 m observed in Egbako indicates favorable conditions for hydrocarbon maturation, making this area promising for petroleum exploration.

Spectral Analysis

Spectral analysis was conducted on the aeromagnetic data of Egbako to estimate the depth to the magnetic basement rocks. This involved dividing the composite aeromagnetic map into 4 overlapping cells (Figure 7). For each block, the radially averaged log-power spectrum was calculated using the MAGMAP filtering tool in Oasis Montaj. The output spectral energy data were used to plot the graph of the logarithm of spectral energy against frequency in cycles per kilometer (Figure 8).

The high-frequency portion of the graph corresponds to shallow magnetic sources, while the low-frequency segment represents deeper magnetic bodies. The slopes of the straight-line segments in both frequency ranges were used to determine the depths of these sources. Shallow magnetic source depths ranged from 0.98-1.51 km, with an average of 1.22 km, whereas deeper sources varied between 3.37 and 4.31 km, averaging 3.77 km (Table 1).

3D Euler Deconvolution

The 3D Euler Deconvolution (ED) method was utilized to estimate the depth to magnetic contacts (Figure 9). A structural index of 0.0, corresponding to a magnetic contact geological model, was applied to the residual map of the study area to identify and determine the depths of magnetic contacts. The estimated depths range from -4.05 to 3807.98 m, with an average depth of 264.07 m.

The study reveals widespread thick sedimentary layers across the study region, with maximum thicknesses of 3.99 km (from SPI), 3.77 km (from spectral analysis), and 3.81 km (from Euler Deconvolution), yielding 73.2% agreement in depth values (Table 2). These significant sediment accumulations surpass the critical depth for hydrocarbon generation (>2.5 km) by 51–60 %. Around 85% of the area contains these thick sediments, with 67% exceeding 2.0 km and 34% exceeding 3.0 km in thickness, while the southwestern regions, such as Enagi, Kutigi, and Ganegi, exhibit shallower sources. These depth intervals correspond to the favourable hydrocarbon generation zone (2.5–4.0 km), where source rocks reach the necessary thermal conditions (60–120 °C) (Adewumi *et al.*, 2017; Ajala *et al.*, 2021). However, no borehole control exists within the study grid; the absence of direct validation is therefore acknowledged as a key limitation and serves as a justification for recommending targeted seismic acquisition to confirm subsurface geometry and stratigraphic continuity. Thus, the area holds strong potential for hydrocarbon exploration. The results from this study conform to the results from Tsepav and Mallam (2017), Salaudeen *et al.* (2025) and Ajama *et al.* (2017).

CONCLUSION AND RECOMMENDATIONS

The depth-estimation results from the three methods — Source Parameter Imaging (SPI), Spectral Analysis, and Standard Euler Deconvolution —indicate promising hydrocarbon potential in approximately 85% of the study area, as they reveal sedimentary thicknesses exceeding 3 km. Such thickness is generally considered adequate for the maturation and accumulation of hydrocarbons. Consequently, the findings of this study should be regarded as reconnaissance evidence warranting seismic follow-up, particularly in zones where sedimentary thickness surpasses 3 km. Conducting more detailed geophysical investigations, such as seismic reflection surveys, in these identified zones will be essential to validate subsurface structures and confirm the presence of potential hydrocarbon-bearing formations.

ACKNOWLEDGEMENT

The authors sincerely thank the Nigerian Geological Survey Agency for providing aeromagnetic data.

REFERENCES

Adebisi, W. A., Folorunso, I. O., Abubakar, H. O., Olatunji, S., & Olaojo, M. O. (2024). Delineating Structural Features Related to Hydrothermal Alterations for Possible Mineralization in Share Area, Kwara State Nigeria Using Aeromagnetic Data. *Indonesian Journal of Earth Sciences, 4*(2), A1265. [Crossref]

Adewumi, T., Salako, K., Salami, M., Mohammed, M., and Udensi, E. (2017). Estimation of Sedimentary Thickness Using Spectral Analysis of Aeromagnetic Data over Part of Bornu Basin, Northeast, Nigeria. *Asian Journal of Physical and Chemical Sciences, 2*(1), 1–8. [Crossref]

Ajala, S. ., Salako, K. A., Rafiu, A. A., Alahassan, U. D., Adewumi, T., and Sanusi, Y. A. (2021). Estimation of Sedimentary Thickness for Hydrocarbon Potential Over Part of Adamawa Trough, Ne Nigeria Using Magnetic Method. *Earth Sciences Pakistan, 5*(1), 01–05. [Crossref]

Ajama, O. D., Hammed, O., Falade, S. C., and Arogundade, A. (2017). Hydrocarbon potentiality of Bida Basin from high resolution aeromagnetic data. *Petroleum and Coal, 59*(6), 991–1007.

Akanbi, E. S., and Udensi, E. E. (2007). Structural trends and spectral depth analysis of the residual field of Pategi Area, Nigeria, using aeromagnetic data. *Nigerian Journal of Physics, 18*(2), 271–276. [Crossref]

Blanco-Montenegro, I., Torta, J. M., Garcia, A., and Arana, V. (2003). Analysis and modelling of the aeromagnetic anomalies of Gran Canaria (Canary Islands). *Earth and Planetary Science Letters, 206*(3-4), 601–616.

Cacace, M., Kaiser, B. O., Lewerenz, B., and Scheck-Wenderoth, M. (2010). Geothermal energy in sedimentary basins: What we can learn from regional numerical models. *Chemie Der Erde, 70*(SUPPL. 3), 33–46. [Crossref]

Dalha, A., Haruna, A. I., & Maigari, A. S. (2024). Geochemical Characterization of Baryte Mineralization in the Gombe Inlier, Gongola Sub-basin, Northern Benue Trough, Nigeria: Insights into Its Origin and Physico-Chemical Conditions. *BIMA JOURNAL OF SCIENCE AND TECHNOLOGY, 8*(4), 165–180. [Crossref]

Ganat, T. A. (2021). *Technical Guidance for Petroleum Exploration and Production Plans* (Issue March). [Crossref]

Ibe Alexander Omenikolo, Terhemba Theophilus Emberga, and Alexander Iheanyichukwu Opara. (2022). Basement depth re-valuation of anomalous magnetic bodies in the lower and middle Benue trough using Euler deconvolution and spectral inversion techniques. *World Journal of Advanced Research and Reviews, 14*(2), 129–145. [Crossref]

Jessop, A. M., and Majorowicz, J. A. (1994). Fluid flow and heat transfer in sedimentary basins. *Geological Society Special Publication, 78*(January 1994), 43–54. [Crossref]

Lawal, T. O., and Nwankwo, L. I. (2017). Evaluation of the depth to the bottom of magnetic sources and heat flow from high resolution aeromagnetic (HRAM) data of part of Nigeria sector of Chad

Basin. *Arabian Journal of Geosciences, 10*(17). [Crossref]

Mark, U. (2019). *Building Local Capacities for the Development of the Nigerian Metals Sector. The 2nd Nigeria Metallurgical Industry Stakeholders' Forum (MISF): Engagement With The Southeast Geopolitical Zone.* [Link]

NGSA. (2009). *Aeromagnetic Datasheets*. Nigeria Geological Survey Agency.

Nwankwo, L. I., and Sunday, A. J. (2017). Regional estimation of Curie-point depths and succeeding geothermal parameters from recently acquired high-resolution aeromagnetic data of the entire Bida Basin, north-central Nigeria. *Geothermal Energy Science, 5*(1), 1–9. [Crossref]

Obaje, N. G. (2009). The Mid-Niger (Bida) Basin. *Geology and Mineral Resources of Nigeria, Lecture Notes in Earth Sciences*, 91–101. [Crossref]

Obaje, N. G., Musa, M. K., Odoma, A. N., and Hamza, H. (2011). The Bida Basin in north-central Nigeria: sedimentology and petroleum geology. *Journal of Petroleum and Gas Exploration Research, 1*(1), 1–013. [Link]

Oghuma, A. A., Obiadi, I. I., and Obiadi, C. M. (2015). 2-D Spectral Analysis of Aeromagnetic Anomalies over Parts of Monguno and Environs, Northeastern Nigeria. *Journal of Earth Science and Climatic Change, 06*(08), 6–11. [Crossref]

Pimentel, N., and dos Reis, R. P. (2020). Nature and Occurrence of Hydrocarbons. In W. Leal Filho, A. M. Azul, L. Brandli, A. Lange Salvia, and T. Wall (Eds.), *Life Below Water* (pp. 1–11). Springer International Publishing. [Crossref]

Rahaman, M. A. O., Fadiya, S. L., Adekola, S. A., Coker, S. J., Bale, R. B., Olawoki, O. A., Omada, I. J., Obaje, N. G., Akinsanpe, O. T., Ojo, G. A., and Akande, W. G. (2019). A revised stratigraphy of the Bida Basin, Nigeria. *Journal of African Earth Sciences, 151*, 67–81. [Crossref]

Saeed, V. V. (2000). *Advanced Digital Signal Processing and Noise Reduction*. In John Wiley and Sons Ltd (2nd Ed).

Salako, K. A. (2014). Depth to Basement Determination Using Source Parameter Imaging (SPI) of Aeromagnetic Data : An Application to Upper Benue Trough and Borno Basin , Northeast , Nigeria. *Academic Research International, 5*(3), 74–86. [Link]

Salaudeen, S. A., Adagunodo, T. A., Busari, A. O., Suleman, K. O., and Sunmonu, L. A. (2025). Depth estimation of the residual field of Patigi Area, Nigeria, using source parameter imaging and spectral depth analysis. *Recent Advances in Natural Sciences Journal, 3*, 1–7. [Crossref]

Salaudeen, S. A., Adagunodo, T. A., Sunmonu, L. A., Suleman, K. O., Ayanbisi, O. W., and Oladapo, O. F. (2024). Assessment of sustainable geothermal potential in Patigi region, North-Central Nigeria. *IOP Conference Series: Earth and Environmental Science, 1428*(1), 1–15. [Crossref]

SDGs. (2015). *17 Sustainable Development Goals*. [Link]

Thurston, J., and Smith, R. (1997). Automatic conversion of magnetic data to depth, dip, and susceptibility contrast using the SPITM method. *Geophysics, 62*, 807–813.

Tijjani, Z. Y., Salako, K. A., Bonde, D. S., and Saleh, A. (2021). Estimation of Sedimentary Layer Thicknesses over Parts of Northern Bida Basin, Nigeria. *IOSR Journal of Applied Geology and Geophysics, 9*(1), 50–59. [Crossref]

Tsepav, M. T., and Mallam, A. (2017). Spectral Depth Analysis of some Segments of the Bida Basin , Nigeria , using Aeromagnetic Data. *J. Appl. Sci. Environ. Manage, 21*(2012), 1330–1335. [Crossref]

Tsepav, M. T., and Mallam, A. (2018). Spectral depth analysis of some segments of the Bida Basin, Nigeria, using aeromagnetic data. *Journal of Applied Sciences and Environmental Management, 21*(7), 1330–1335. [Crossref]